# A STUDY FOR THE POTENTIAL OF AMMONIA-WOOD CHARCOAL ADSORPTION REFRIGERATION SYSTEM

by

**WONG CHEE KHOON**

**Thesis submitted in fulfillment of the requirements**
**for the degree of**
**Master of Science**

**March 2012**

# ACKNOWLEDGEMENT

I would like to express my gratitude to Prof. Horizon Walker Gitano-Brigss for his utmost guidance, encouragement, advices and patience that led to the completion of this work. His words of encouragement had brought me further than I have ever achieved.

Also, I would like to extend my gratitude to all technicians for assisting me in the project be it advices or hands-on help. Here, I would take this opportunity to thank Mr. Azhar, Mr. Khomaruddin, Mr. Latif and Mr. Kamarul for their special attention and assistance.

Never to forget my fellow friends, Mr. Teoh Yew Heng, Mr. Chuah Hun Guan, Mr. Khoo Aik Soon, Mr. Loh Jian Haur, Mr. Chong Chuong Leong, Mr. Ahmad Syazli, Mr. Lee Ying Wei, Mr. Goh Chin Yuan, Mr. Tan Wei Hong and Mr. Lim Kar Loon for being with me in times of troubles, listening to my rants and encouraging me to persevere. I cherish the moments of laughter and joy for time we shared together despite our business. I appreciate it a lot!

Finally, I am thankful for the God that He provides and helped me to endure throughout; allow things to happen so that I may learn from it. Each day, I am thankful that only through Him I can persevere to the end. Also, to my mother, who endure her own time alone at home, while I am away to accomplish this task, God bless you. Her approval and encouragement has brought me closer to the ending line each day.

Thanks!

# TABLE OF CONTENTS

**ACKNOWLEDGEMENT** **ii**

**TABLE OF CONTENTS** **iii**

**LIST OF TABLES** **vii**

**LIST OF FIGURES** **viii**

**LIST OF ABBREVIATIONS** **x**

**NOMENCLATURES** **xi**

**ABSTRAK** **xvi**

**ABSTRACT** **xvii**

**CHAPTER 1 INTRODUCTION** **1**

1.0 Research Background 1

1.1 Objectives 4

1.2 Scope of Research 4

**CHAPTER 2 LITERATURE REVIEW** **5**

2.0 Overview 5

2.1 Adsorption on Solid Surface 5

2.2 Wood Charcoal as an Adsorbent 8

2.3 Ammonia as Refrigerant 11

2.4 Adsorption of Ammonia on Carbon 13

2.5 Ammonia-Activated Carbon Adsorption Refrigeration 18

2.6 Summary 28

**CHAPTER 3 MATERIALS AND METHODOLOGY 30**

3.0 Overview 30

3.1 Flow chart 31

3.2 Study of wood charcoal 32

3.2.1 Wood Charcoal 32

3.2.2 Adsorption study of ammonia on wood charcoal 35

3.2.3 Desorption study of ammonia on wood charcoal 40

3.3 Design of adsorption refrigeration 43

3.3.1 An Ideal Refrigeration Cycle 43

3.3.2 Overall thermodynamic analysis 44

3.3.3 Adsorbate and Adsorbent analysis 47

3.3.4 Heat exchanger analysis for corrugated louver fins 47

3.3.4.1 Condenser analysis 50

3.3.4.2 Evaporator analysis 52

3.4 Summary 57

**CHAPTER 4 RESULTS AND DISCUSSION 58**

4.0 Overview 58

4.1 Study of wood charcoal 58

4.1.1 Wood Charcoal 58

4.1.2 Transient adsorption study of ammonia on wood charcoal 62

4.1.3 Desorption study of ammonia on wood charcoal 67
4.2 Thermodynamic analysis of adsorption refrigeration 70
4.2.1 Adsorbate and Adsorbent analysis 71
4.3 Wood charcoal selection for ammonia-wood charcoal refrigeration system 73
4.4 Heat exchanger analysis for corrugated louver fins 75
4.5 Error analysis 77
4.6 Summary 81
**CHAPTER 5 CONCLUSION 82**
5.1 Conclusion 82
5.1.1 Properties and characteristics of wood charcoal. 82
5.1.2 Adsorption and desorption characteristics of ammonia on wood charcoal. 82
5.1.3 The adsorption refrigeration system of 1kW cooling power 83
5.2 Future work 83
**REFERENCES 85**
**BIBLIOGRAPHY 90**
**APPENDICES 92**

Appendix 1: Reactor design

Appendix 2: Thermophysical properties of Ammonia

Appendix 3: Thermophysical properties of Superheated Ammonia

Appendix 4: Condenser analysis

Appendix 5: Evaporator analysis

Appendix 6: Adsorber analysis

Appendix 7: Desorber analysis

Appendix 8: Dimensionless number

Appendix 9: Thermodynamic analysis on adsorption refrigeration system using wood charcoal

Appendix 10: Adsorbate-Adsorbent requirement analysis

Appendix 11: Analysis of the adsorption refrigeration system using activated carbon for the same working condition for wood charcoal type B.

# LIST OF TABLES

Table 2.1 Properties of common refrigerants in adsorption refrigeration. ............... 13

Table 2.2 Characteristics of granulate carbon adsorbent in Dubinin-Radushkevich equation. ............... 15

Table 2.3 Characteristics and adsorption energy for ammonia on chemically activated carbon ............... 16

Table 2.4 Performance and capability of various ammonia-activated carbon adsorption refrigeration systems ............... 23

Table 4.1 Characteristics of different sizes of wood charcoal ............... 59

Table 4.2 Temperatures and mass adsorb for adsorption of ammonia on 180 g wood charcoal at one bar gauge pressure. ............... 64

Table 4.3 Integral heat of adsorption of ammonia on wood charcoal at one bar gauge pressure ............... 66

Table 4.4 Characteristics of desorption of ammonia from wood charcoal at high temperatures. ............... 69

Table 4.5 Analytical results for thermodynamic analysis of the adsorption refrigeration system ............... 71

Table 4.6 Mass of adsorbate-adsorbent required for the type of granulate wood charcoal ............... 72

Table 4.7 Comparison of properties for the adsorption refrigeration system using wood charcoal type B and C ............... 73

# LIST OF FIGURES

Figure 2.1 The structure of activated carbon which resembles graphite ...... 10

Figure 2.2 Structure of ammonia with lone electrons on the top edge of trigonal pyramid ...... 13

Figure 2.3 Ammonia adsorption of chemically activated wood based carbon at relative low pressure ...... 17

Figure 2.4 Thermodynamic cycle of a basic adsorption refrigeration. A, P-T-x diagram and B, Schematic diagram. ...... 19

Figure 3.1 Flow chart for the research on the design of an adsorption refrigeration system using ammonia and wood charcoal. ...... 31

Figure 3.2 Cone crusher machine ...... 33

Figure 3.3 Timed-sieve shaker machine ...... 34

Figure 3.4 Data acquisition unit, Agilent U2351 with 16 analogue input channel ...... 35

Figure 3.5 Cross section illustration of the reactor filled with charcoal. Temperatures were taken at the indicated thermocouple locations. ...... 37

Figure 3.6 Schematic of adsorption experimental setup. ...... 38

Figure 3.7 Deviation of the mass scale reading and loaded with calibrated masses ...... 39

Figure 3.8 Schematic of desorption experimental setup**.** ...... 42

Figure 3.9 Pressure-enthalpy diagram for an adsorption cycle. ...... 43

Figure 3.10 Definition of geometrical parameters of corrugated louver fins. ...... 49

Figure 3.11 Film condensation in a horizontal tube. A-cross section view for low flow vapor velocities. B-longitudinal view for large vapour velocities. ...... 51

Figure 3.12 Flow patterns in a horizontal tube evaporator. $x$ is the quality of the fluid ...... 54

Figure 4.1 Inner temperature profile for ammonia adsorption at one bar gauge pressure ...... 63

Figure 4.2 Mass of ammonia absorb per unit mass of wood charcoal at one bar gauge pressure ...... 64

Figure 4.3 Pressure in the reactor representing the mass desorbed from wood charcoal for various temperature. .......... 68

Figure 4.4 The time variant error of mass of the adsorption equipment setup. .......... 77

Figure 4.5 Min-Max-Average plot for temperature of the inner reactor during the adsorption experiment .......... 78

Figure 4.6 Min-Max-Average plot for temperature of the reactor wall during the adsorption experiment .......... 79

Figure 4.7 Min-Max-Average plot for temperature of the mass adsorb during the adsorption experiment .......... 80

Figure 4.8 Measurement error for pressure transmitter in the desorption experiment for both type of wood charcoal .......... 81

# LIST OF ABBREVIATIONS

ODP : Ozone depletion potential

GWP : Global warming potential

IUPAC : International Union of Pure and Applied Chemistry

$NH_3$ : Ammonia

C : Carbon

DR : Dubinin-Raduskevich

H : Hydrogen

O : Oxygen

N : Nitrogen

S : Sulfur

AC : Activated carbon

CFC : Chlorofluorocarbons

HFC : Hydrofluorocarbons

HCFC : Hydrochlorofluorocarbons

ASHRAE : American Society of Heating, Refrigerating and Air-Conditioning Engineers

SEM : Scanning Electron Microscope

EDX : Energy-dispersion X-ray spectroscopy

BET : Brunauer-Emmett-Teller

COP : Coefficient of performance

SCP : Specific cooling power

# NOMENCLATURES

| **Symbols** | **Definition** | **Unit** |
|---|---|---|
| $A$ | total heat transfer area | $m^2$ |
| $A_c$ | cross section of flow area | $m^2$ |
| $A_{HX}$ | area for heat exchanger | $m^2$ |
| $A_{cell}$ | total heat transfer surface area in a cell | $m^2$ |
| $A_{f,cell}$ | cell fin surface area | $m^2$ |
| $A_{fr,cell}$ | cell frontal area | $m^2$ |
| $A_{o,cell}$ | cell free-flow area | $m^2$ |
| $A_o$ | free flow area | $m^2$ |
| $A_{p,cell}$ | cell primary (tube) surface area | $m^2$ |
| $A_{w,cell}$ | wall conduction area per unit cell | $m^2$ |
| $b$ | vertical fin height | mm |
| $c_p$ | specific heat capacity | $kJ\ kg^{-1}\ K^{-1}$ |
| $C_{p,AC}$ | specific heat capacity for activated charcoal/wood charcoal | $kJ\ kg^{-1}\ K^{-1}$ |
| $C_{p,NH_3}$ | specific heat capacity for ammonia | $kJ\ kg^{-1}\ K^{-1}$ |
| $C_{p,l}$ | specific heat capacity of the fluid in liquid phase | $kJ\ kg^{-1}\ K^{-1}$ |
| $C_{p,v}$ | specific heat capacity of the fluid in vapour phase | $kJ\ kg^{-1}\ K^{-1}$ |
| D | coefficient of Dubinin-Radushkevich equation in the pressure form | - |
| $D_h$ | hydraulic diameter | m |
| $F$ | convective boiling enhancement factor | - |
| $G$ | fluid mass velocity on minimum free area | $kg\ m^{-2}\ s^{-1}$ |

| **Symbols** | **Definition** | **Unit** |
|---|---|---|
| $g$ | gravity acceleration, 9.81 m $s^{-2}$ | m $s^{-2}$ |
| $H_t$ | tube outside width | mm |
| $\boldsymbol{h}$ | enthalpy | kJ $kg^{-1}$ |
| $h$ | heat transfer coefficient | W $m^{-2}$ $K^{-1}$ |
| $h'_{fg}$ | modified latent heat | kJ $kg^{-1}$ |
| $h_{cb}$ | heat transfer coefficient for convective boiling | W $m^{-2}$ $K^{-1}$ |
| $h_{LO}$ | liquid heat transfer coefficient | W $m^{-2}$ $K^{-1}$ |
| $h_{nb}$ | heat transfer coefficient for nucleate boiling | W $m^{-2}$ $K^{-1}$ |
| $h_{TP}$ | heat transfer coefficient for two phase boiling | W $m^{-2}$ $K^{-1}$ |
| $j$ | Colburn factor | - |
| $\boldsymbol{k}$ | coefficient of Dubinin-Radushkevich equation | |
| $k$ | thermal conductivity | W $m^{-1}$ $K^{-1}$ |
| $k_l$ | thermal conductivity of the fluid in liquid phase | W $m^{-1}$ $K^{-1}$ |
| $k_v$ | thermal conductivity of the fluid in vapour phase | W $m^{-1}$ $K^{-1}$ |
| $l_l$ | louver cut length | mm |
| $L_f$ | fin plate width | mm |
| $l_p$ | louver pitch | mm |
| $\dot{m}$ | mass flowrate | kg $s^{-1}$ |
| $\dot{m}_{refrigerant}$ | refrigerant mass flow rate | kg $s^{-1}$ |
| $m_{AC}$ | mass of activated charcoal/wood charcoal | kg |
| $m_a$ | mass of adsorbate adsorbed | kg |
| $m_{bed}$ | mass of adsorbent bed | kg |

| **Symbols** | **Definition** | **Unit** |
|---|---|---|
| $m_m$ | mass of adsorbent in the system | kg |
| $m_s$ | measured mass | kg |
| n | coefficient of Dubinin-Radushkevich equation | - |
| $Nu$ | Nusselt number | - |
| p | pressure | Pa |
| $p_f$ | fin pitch | mm |
| $Pr$ | Prandtl number | - |
| $p_{sat}$ | saturation pressure | Pa |
| $p_t$ | tube pitch | mm |
| $P_w$ | wetted perimeter | m |
| $Q_{cond}$ | Heat rate to be released in condenser | W |
| $Q_{evap}$ | Heat rate to be absorb in evaporator | W |
| $Re_{lp}$ | Reynolds number based on the louver pitch $l_p$ | - |
| $Re$ | Reynolds number | - |
| S | suppression factor | - |
| $St$ | Stanton number | - |
| t | thickness | m |
| T | temperature | K |
| $T_e$ | excess temperature | K |
| $T_s$ | wall surface temperature | K |
| $T_{sat}$ | saturation temperature | K |
| $U$ | overall heat transfer coefficient | $W\ m^{-2}\ K^{-1}$ |
| $u_m$ | mean fluid velocity | $m\ s^{-1}$ |

| Symbols | Definition | Unit |
|---|---|---|
| $v_a$ | volume occupied by adsorbed mass | $m^3$ |
| $v_{max}$ | limiting volume occupied by adsorbed mass | $m^3$ |
| $V_{cell}$ | cell volume | $m^3$ |
| $W_t$ | tube outside width | mm |
| $x$ | equilibrium amount adsorbed | - |
| $\boldsymbol{x}$ | quality of the mixture | - |
| $x_0$ | limiting amount adsorbed | - |
| $X_{tt}$ | Martinelli parameter | - |
| | | |
| $\Delta G$ | Gibbs energy | J |
| $\Delta p_v$ | pressure difference from Claypeyron equation | Pa |
| $\Delta S$ | Entropy | $J\ K^{-1}$ |
| $\Delta H$ | Heat of adsorption | J |
| $\beta$ | surface area density | $m^{-1}$ |
| $\delta$ | fin thickness | mm |
| $\theta$ | louver angle | ° |
| $\theta_B$ | wall superheat | K |
| $\rho$ | density | $kg\ m^{-3}$ |
| $\rho_l$ | density of the fluid in liquid phase | $kg\ m^{-3}$ |
| $\rho_v$ | density of the fluid in vapour phase | $kg\ m^{-3}$ |
| $\mu$ | dynamic viscocity | Pa.s |
| $\mu_l$ | dynamic viscosity of the fluid in liquid phase | Pa.s |
| $\mu_v$ | dynamic viscosity of the fluid in vapour phase | Pa.s |

| **Symbols** | **Definition** | **Unit** |
|---|---|---|
| $\sigma$ | surface tension | N $m^{-1}$ |
| $\boldsymbol{\sigma}$ | ratio of free flow area to frontal area | - |
| $\sigma_h$ | Hoop stress | Pa |
| $\sigma_l$ | Longitudinal stress | Pa |

# KAJIAN POTENSI AMMONIA-ARANG KAYU UNTUK SISTEM PENDINGINAN PENJERAPAN

## ABSTRAK

Sistem penjerapan telah mendapat tumpuan berbanding sistem pemampatan wap kerana ciri mesra alam, potensi penipisan ozon sifar dan potensi pemanasan global sifar. Meskipun terdapat banyak penyelidikan tentang penjerapan dan nyahjerap amonia pada karbon teraktif, namun hanya sedikit yang ditemui untuk arang kayu. Dalam kajian ini, arang kayu tempatan diperoleh, dihancur dan diayak kepada tiga ukuran partikel. Ukuran partikel 1.18-3.35 mm menunjukkan luas permukaan tentu yang tertinggi iaitu 155.37 $m^2$ $g^{-1}$ dengan isipadu spesifik 0.1309 $cm^3$ $g^{-1}$ dan purata diameter liang sebanyak 2.503 nm. Kemudian, cara gravimetri digunakan untuk mengkaji penjerapan amonia pada arang kayu sebagai fungsi suhu, masa dan jisim. Cara tersebut terbukti jitu dan murah untuk dibina. Untuk penelitian nyahjerap, cara barometrik digunakan untuk mempelajari nyahjerap amonia dengan suhu. Penjerapan amonia pada arang kayu menghasilkan purata jerapan 0.081 g $NH_3$ $g^{-1}$ C manakala penelitian nyahjerap menunjukkan jumlah nyahjerap adalah hanya 20 hingga 21 % daripad amaun jerapan pada julat suhu 162 hingga 202 ° C. Sistem pendingin jerapan direkabentuk untuk kapasiti penyejukan 1 kW. Dari hasil analisis tersebut, sistem mengandungi 1.83 kg arang kayu dan 93.57 g gas amonia dengan COP 0.40 dan SCP ialah 0.546 kW $kg^{-1}$.

# A STUDY FOR THE POTENTIAL OF AMMONIA-WOOD CHARCOAL ADSORPTION REFRIGERATION SYSTEM

## ABSTRACT

Adsorption systems have gained popularity over vapour compression system due to their being environmentally benign, having zero ozone depletion potential and zero global warming potential. Despite much research on the adsorption and desorption of ammonia on activated carbon, relatively few reports were found for wood charcoal. In this study wood charcoal, obtained locally, was crushed and sieved into three particle sizes for study. Particles sized 1.18 to 3.35 mm yielded the highest specific surface area which of 155.37 $m^2\ g^{-1}$ with specific volume of 0.1309 $cm^3\ g^{-1}$ and an average pore diameter of 2.503 nm. An innovative gravimetric method was used to characterize the adsorption of ammonia on the wood charcoal as a function of temperature, mass and time. Such method was found to be accurate and inexpensive to fabricate. For desorption study, a barometric method was employed to study the desorption of ammonia at various temperature. Adsorption of ammonia on wood charcoal yields an average of 0.081 $g\ NH_3\ g^{-1}\ C$ adsorbed while the desorption study shows an amount desorbed only 20 to 21% of the amount adsorbed at temperatures of 162 to 202 °C. An adsorption refrigeration system was designed for a 1 kW cooling capacity. From the analysis, the system consists of 1.83 kg of wood charcoal and 93.57 g of ammonia gas with a COP of 0.40 and SCP of 0.546 $kW\ kg^{-1}$.

# CHAPTER 1 INTRODUCTION

## 1.0 Research Background

Concern over harmful environmental side effects of vapour compression cooling and the regulation made in Montreal Protocol 2006 to phase out such refrigerants have led many researchers to search for alternative cooling methods to replace such cycle. CFCs, HFCs and HCFCs used in vapour compression cooling are major contributors to ozone layer depletion and global warming. Over the years, adsorption cooling has received the attention of many researchers because of its ability to utilize relatively low quality heat to drive the cycle. The ability to use natural refrigerants as alternatives to CFCs, HCFCs or HFCs implies that adsorption cooling systems can be environmentally benign, having zero ozone depletion potential (ODP) as well as zero global warming potential (GWP). The working pairs of such system are mainly silica gel water, zeolite-water, activated carbon-ammonia, activated carbon-methanol and activated carbon fiber-ammonia. Since adsorption cooling systems utilize low heat sources as the main driving power, waste heat and even solar heating can be used to operate the systems (Vasilieve et al., 2001 ). Other sources can be exhaust gas heat from internal combustion engines and geothermal power. With the elimination of the mechanical compressor, the system does not require moving parts for circulation of the refrigerant. Thus, the system operates without noise or vibration.

Despite the toxicity and flammability of ammonia, it has been used for over 100 years in the field of refrigeration. Experience and refinements in the field of ammonia refrigeration have generated a clear understanding and countermeasures for dealing with ammonia. Reliable exposure charts have been developed for workers who deal with ammonia in their working environment (Lindborg, 2006). On these charts, the acceptable exposure limit to ammonia is plotted as a function of time and concentrations. Personnel working with ammonia are able to use the chart as an exposure guideline when dealing with ammonia. Of the common refrigerants, ammonia has the highest latent heat (1357 kJ kg$^{-1}$) after water (2258 kJ kg$^{-1}$) (ASHRAE, 2005). Water has a major limitation due to its tendency to crystallize below 0°C. Cooling systems with ammonia as the refrigerant typically do not operate at sub-ambient pressures. This allows simplified construction and higher reliability than sub-ambient pressure systems. Leaks can be easily detected from the characteristic odor of ammonia. Common materials, such as aluminium and stainless steel, can be used in the construction of such systems, however ammonia is corrosive to copper and its alloys. Wang et al. (2009) compared working pairs of ammonia-activated carbon and methanol-activated carbon. They showed that the former has better mass transfer because of its higher working pressure for the same temperature. The cycle time for the ammonia-activated carbon is therefore faster compared to methanol-activated carbon because of its high mass transfer rate.

Meanwhile, activated carbon is well known for its ability to absorb substances. Having a high surface area per unit mass, activate carbon provides a large area for adsorption. Therefore, it has been used in many applications such as removal of undesirable odor, colour, taste, organic and inorganic impurities, air purification, pharmaceuticals, industrial gas masks and others. Activated carbon typically has a specific surface area of 500 to 2500 m$^2$ g$^{-1}$ (Bansal and Goyal, 2005 and Keller and Staudt, 2005). Activated carbon has also attracted interest in adsorption cooling system due to its ability to adsorb ammonia. Lee and Reucroft (1999c) reported that activated carbon has a stronger adsorption interaction with ammonia compared to carbon tetrachloride, acetone and hydrogen sulfide. Activated carbon can be synthesized from wood. Physically activated carbon is produced by exposing the raw material to an atmosphere of air, $CO_2$ or steam in the temperature range of 800°C to 900°C while chemically activated carbon is soak into oxidizing agent such as phosphoric acid (Bansal and Goyal, 2005). In an attempt to increase the adsorption of ammonia on activated carbon, Oliveira et al. (2007) introduce calcium chloride on the carbon to enhance its adsorption. Since activated carbon is produced by a more laborious process than wood charcoal, wood charcoal could be a less expensive alternative to activated carbon due to its relatively simple production. The cost of wood charcoal is RM 1.40 per kg while activated carbon cost approximately RM5.47 per kg (Aziz et al., 2006). As activated carbon cost four times more than wood charcoal, wood charcoal may be a lower cost alternative to activated carbon.

The ammonia-activated carbon adsorption pair has been studied by many researchers for its application in adsorption cooling (Tamainot-Telto and Critoph, 2003, Critoph, 1996, Tamainot-Telto and Critoph, 1997, Pearson, 2008; Al Mers et al., 2006). As reported in the review carried out by Demir et al. (2007) the ammonia-activated carbon adsorption pair was able to achieve a COP in the range of 0.30 to 0.62. However, most of the work was based on numerical modeling and simulated data. Most ammonia-activated carbon adsorption cycles require very low heat input for refrigerant regeneration. Typical regeneration temperatures are 60°C or greater. Heat sink temperatures for the adsorption cycle are as high as 30°C. Despite much research on the ammonia-activated carbon pair, there are no specific mathematical equations for calculating the properties of adsorption either by statistical methods or by phenomenological methods (Keller and Staudt, 2005).

## 1.1 Objectives

The objectives of this research work are as follows:

1. To identify the properties and characteristics of wood charcoal.
2. To study the adsorption and desorption characteristics of ammonia on wood charcoal.
3. To design the adsorption refrigeration system of 1kW cooling power using analytical approach.

## 1.2 Scope of Research

The scope of this research work is as follows:

1. Study on properties of local mangrove wood charcoal ground to three different sizes.
2. Experimentally investigate the adsorption of wood charcoal at low pressure with a simple experiment test setup using gravimetric method. This work also involves setting up data acquisition hardware and software, for programming data logging and analysis purpose.
3. Desorption is experimentally investigated using a barometric method to identify the amount to mass desorb compared with a control experiment. Desorption study is based on the temperature variation of the wood charcoal.
4. Design of an adsorption refrigeration system of 1kW cooling power using experimental data from the adsorption-desorption study together with fundamentals of thermodynamics and heat transfer. Ready-made heat exchanger will be studied for its suitability in this project contrary with fabrication of a new custom heat exchanger.

# CHAPTER 2 LITERATURE REVIEW

## 2.0 Overview

In this chapter, the introduction of basic principles of adsorption on solids are reviewed, followed by the adsorbent properties of activated carbon and comparison with wood charcoal. The use of ammonia as refrigerant and adsorption on wood charcoal is also discussed. An ideal refrigeration system is introduced before explaining the adsorption refrigeration system using ammonia and activated carbon.

## 2.1 Adsorption on Solid Surface

Adsorption is a phenomenon where the concentration of a gas or liquid on the solid surface is higher than the bulk when such gas or liquid comes in contact with a solid surface. Adsorption is a spontaneous process. The constituent that is attached to the surface is called adsorbate while the constituent to which it attached is called adsorbent. When the solid surface of adsorbent is exposed to the adsorbate, the molecules of the adsorbate will strike on the surface of the adsorbent. Some will be adsorbed unto the surface while some will be rebound back to the bulk gas or liquid. Initially, the adsorption rate is very high due to the bare surface for adsorption. As more adsorption sites are covered with adsorbate, the available surface for adsorption decreases and adsorption rate reduces. Simultaneously the desorption rate increases because desorption takes place at the place where adsorbent surface covered by adsorbate. As time passes, the rate of adsorption continues to fall while the rate of desorption increases until an equilibrium is reached. Amount adsorbed can is defined by mass of adsorbate, $m_a$ and mass of adsorbent, $m_m$. The equilibrium amount adsorbed, $x = {}^{m_a}/_{m_m}$ is a function of pressure and temperature (Ponec et al., 1974); i.e.,

$$x = \frac{m_a}{m_m} = f(p, T) \tag{2.1}$$

When gas or liquid is adsorbed on the surface of an adsorbate, molecules of such adsorbate have fewer degrees of freedom than in the bulk gas or liquid. This results in a decrease in entropy, ΔS, during adsorption. Using thermodynamic relationship, i.e. Gibbs energy, ΔG,

$$\Delta G = \Delta H - T\Delta S \tag{2.2}$$

It follows that the term $\Delta H$, which is the heat of adsorption, must be negative for a spontaneous process. This shows that adsorption is an exothermic process though some cases of adsorption are endothermic. An example of endothermic adsorption is adsorption of hydrogen on glass. There are two types of adsorption, namely physical adsorption or physisorption and chemical adsorption or chemisorptions. The major characteristic differentiating these type of adsorption is the manner to which adsorbate is attached to adsorbent, which is the bonding force. In physisorption, constituents are bonded with weak forces such as van der Walls force while chemisorptions involves exchange or sharing of electrons between adsorbent and adsorbate. The latter has higher bonding force. Another common difference between two kinds of adsorption is the magnitude of the heat of adsorption. In the case of physisorption, the heat of adsorption does not usually exceed 10 to 20 kJ per mole and it is on the same order of heat of condensation. For the case of chemisorptions, the heat of adsorption is usually ranges from 40 to 400 kJ per mole (Bansal and Goyal, 2005; Keller and Staudt, 2005). However, in some cases the heat of adsorption in chemisorptions does not significantly differ from physisorption. Physisorption does not require activation energy where else chemisorptions requires activation energy.

As adsorption is an exothermic process, heat is released to the surroundings. Heat of adsorption is expressed in two ways, i.e. integral heat of adsorption and differential heat of adsorption. Integral heat of adsorption is the total amount of heat released when one gram of an out gassed solid adsorbs an amount of adsorbate, $m_a$. It is commonly expressed as Joules per gram of the adsorbent together with the amount adsorbed per unit adsorbent. Another type of heat of adsorption is called differential heat of adsorption or isosteric heat of adsorption, which is commonly expressed as Joules per mole of adsorbate. This is the heat evolved when the adsorbent, which had already adsorbed an amount of adsorbate, adsorbs an additional amount of $\Delta m_a$.

From the work of Dubinin and Radushkevich (1947) integrated with Polanyi's potential theory, adsorption on microporous yields an equation which is called Dubinin-Radushkevich equation. This equilibrium equation is regarded as most fundamentally sound and widely used and accepted for physisorption on solids (Wang et al., 2009).

$$v_a = v_{max}\ exp\left[-D\left(T\ \ln\left(\frac{p_{sat}}{p}\right)\right)^n\right] \tag{2.3}$$

where $v_a$ is the volume occupied by adsorbed mass, $v_{max}$ is the limiting volume occupied by adsorbed mass, D is the coefficient of Dubinin equation in the pressure form, n is a coefficient, p is pressure of the equilibrium where as $p_{sat}$ is the saturation pressure at temperature T. With the Clausius-Clayperon equation relating temperature and pressure for saturated adsorbate, the Dubinin-Radushkevich equation yields (Teng et al., 1997).

$$x = x_o \exp\left[-\boldsymbol{k}\left(\frac{T}{T_{sat}} - 1\right)^n\right] \tag{2.4}$$

The saturation temperature, $T_{sat}$ corresponds to the saturation pressure, $P_{sat}$. In most cases, the Dubinin-Radushkevich equation of the later form is used which corresponds to the direct measurement of mass adsorbed by a known mass of adsorbent. Coefficients D, **k** and n differ for each type of adsorption pair and also the characteristics of the adsorbent-adsorbate as well.

## 2.2 Wood Charcoal as an Adsorbent

Ideally, an adsorbent has a high surface area per unit mass, a high concentration of active sites for adsorption and a porous structure to adhere adsorbate. Activated carbon is popular for use as an adsorbent in many applications. Generally, activated carbon has a specific surface area in the range of 500 to 2500 $m^2 g^{-1}$ (Keller and Staudt, 2005; Bansal and Goyal, 2005). Activated carbon is prepared via two stages. First, the raw carbonaceous material is exposed to temperatures up to 700 $^oC$ in an inert environment. This process is called carbonization. Next, the carbonized material will undergo an activation process whereby it is either treated through physical activation or chemical activation. For physical activation, carbonized material is exposed to a high temperature condition of air, carbon dioxide or steam. Physical activation temperatures range from 800 to 900 $^oC$ (Bansal and Goyal, 2005; Keller and Staudt, 2005). Under such conditions, non-carbon elements such as oxygen, hydrogen and nitrogen are largely removed leaving mostly carbon and where pores are also developed in the material during this process. Chemical activation is a process where oxidizing chemicals are used to remove residual elements in the carbonized material. Phosphoric acid is one of the common agents used in chemical activation (Keller and Staudt, 2005). It is performed by soaking the carbonized material in an aqueous solution of the agent.

Although the objective of physical or chemical activation process is to remove non-carbon elements from the carbonaceous material, traces of non-carbon elements still remain. A typical activated carbon is found to have an elemental composition of 88% C, 0.5% H, 0.5% N, 1%S and 6 to 7% O with the balance representing inorganic ash constituents (Bansal et al., 2005; Rodriguez-Reinoso, F., 2006).

During the carbonizing process, residual elementary carbon atoms arranged themselves into stacks of flat, aromatic sheets cross linked in a random manner. Irregular arrangements of aromatic sheets leave free interstice. With these free interstices, pores are formed within which makes the activated carbons are excellent adsorbents. Specific pore volumes ranges from 0.20 to 0.60 $cm^3$ $g^{-1}$ (Bansal and Goyal, 2005; Marsh, H. and Rodriguez-Reinoso, F., 2006). Activated carbons have associated with pores of various sizes, from less than a nanometer to several thousand nanometers. Dubinin (1960) proposed a classification of pores according to their size. Such classification is now accepted by the International Union of Pure and Applied Chemistry (IUPAC). The pores are classified into three groups according to their width, which represents the radii of the pore. The groups are namely micropores, mesopores and macropores. Micropores are pores with effective diameter of less than 2 nm. These micropores contribute about 95% of the total internal surface area where adsorption takes place. Mesopores have diameters ranging from 2 to 50 nm. The surface area of these pores do not exceed 5% of the total internal surface area. These pores act as conduits for molecules to enter into inner pores for adsorption. Macropores enable molecules to pass rapidly to smaller pores situated deeper within the carbon. Macropores are found typically at the surface of the carbon particle. Diameter of macropores are more than 50 nm and they contribute relatively little surface area.

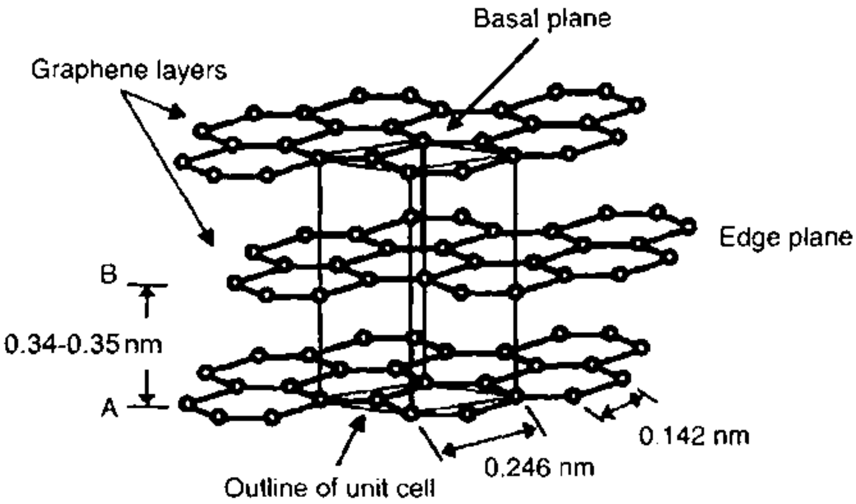

Figure 2.1 The structure of activated carbon which resembles graphite (Marsh and Rodriguez-Reinoso, 2006)

Activated carbon has a microcrystalline structure which resembles graphite but the interlayer spacing ranges from 0.34 to 0.35 nm in activated carbon compared to 0.335 nm in graphite (Marsh and Rodriguez-Reinoso, 2006). These crystalline structures start to build up during the carbonizing process. Layers of aromatic sheets have less order of arrangement compared to graphite. The variation of the arrangement is due to the imperfect or partially burnt layers. This results in the existence of unpaired electrons and incompletely saturated valances. Such locations readily form bonds with other groups or elements via either chemical bonding or physical bonding. This attribute enhances the adsorption properties of activated carbon (Marsh and Rodriguez-Reinoso, 2006).

Adsorption properties inherent in activated carbon have led to its widespread utilization as an adsorbent. Activated carbon is used to remove organic substances from gases and purification of natural gas, biogas and many others. Further applications include deodorization of air, filter media in gas masks, agent for waste water purification and storage of gases. One interesting application of activated carbon is for the adsorption of ammonia. Ammonia is a common type of refrigerant in refrigeration systems. Activated carbon can be used to replace water of aqua-ammonia absorption refrigeration system. Huang et al. (2008) tested the adsorption of ammonia on various activated carbons. In their report, ammonia adsorption capacity ranging from 2.3 to 41.6 mg $NH_3$ $g^{-1}$ AC. Lee and Reucroft (1999c) introduce a correlation on adsorption capacity with average pore diameter and surface oxygen group. In their findings, adsorption capacity is significantly influenced by the average pore diameter at low relative pressure due to narrower walls of micropores. Smaller micropore size has higher adsorption potential due to narrower walls of micropores.

Similarly, mangrove wood charcoal is prepared by heating of wood at high temperature in a kiln with burning mangrove wood as fuel. The kiln is kept hot for 8 to 10 days depending on the capacity of the kiln. Burning of wood in the kiln by drawing fresh air from outside the kiln provides a suitable atmospheric condition for carbonizing and oxidizing of wood into activated carbon. Therefore, wood charcoal resembles the properties of activated charcoal in many ways. However, properties have yet to be investigated. The cost of wood charcoal is at RM 1.40 per kg while activated carbon cost approximately RM5.47 per kg (Aziz et al., 2006). As, activated carbon cost four times more than a wood charcoal, wood charcoal may be a lower cost alternative to activated carbon.

## 2.3 Ammonia as Refrigerant

Ammonia is widely used as a refrigerant in large refrigeration plants such as ice plants, breweries, and industrial processing plants. Ammonia has been used as refrigerant for over 160 years since its first use in around 1850s (ASHRAE, 2006).

Experience and refinements in the field of ammonia refrigeration have generated a clear understanding and countermeasures in dealing with ammonia as it is a toxic compound. Due to its toxicity, ammonia is not allowed as a refrigerant in direct air-conditioning system for human comfort, but it can be used as a refrigerant in chillers where the chilled water is pumped to air handling units (Pearson, 2008). In addition, ammonia is corrosive to copper or copper based materials. Therefore, components of system of this refrigerant should not be made of copper to avoid leakage. This ranges from pipes and fittings to valves and bearings. Ammonia leakage can be easily detected due to its irritating odour as compared to other common refrigerants which are odourless. Properties of common refrigerants are tabulated in Table 2.1. The main advantage of ammonia over other common refrigerants is its high latent heat, which is 1357 kJ kg$^{-1}$ (Ameen, 2006, ASHRAE, 2006; Owen, 2005). This allows a high amount of heat per mass of refrigerant to be adsorbed during vaporization of liquid ammonia. This will result in a high cooling capacity. Furthermore, ammonia has zero global warming potential as well as ozone depletion potential (Wang, et al., 2009). Thus, this satisfies the regulation made during Montreal Protocol 2006 which allows the continuation of ammonia as a refrigerant while other CFCs and HCFCs are to be phased out in due time. In addition, the freezing point of ammonia, -77.7 $^{o}$C, is low enough for ordinary refrigerating temperatures. Although ammonia will burn in narrow range of high concentrations, it is difficult to ignite (ASHRAE, 2006). Vandebroek et al. (2002) concluded that the most ignitable mixtures of ammonia and air is at 50 mol% ammonia, which is also two to three times of the stoichiometric value. Additionally, auto-ignition was only possible when the temperature is above 550 $^{o}$C.

Table 2.1 Properties of common refrigerants in adsorption refrigeration.

| **Refrigerants** | **Chemical formula** | **Normal boiling point, °C** | **Freezing point, °C** | **Molecular weight, g mol$^{-1}$** | **Latent heat of vaporization, kJ kg$^{-1}$** | **Density, kg m$^{-3}$** |
|---|---|---|---|---|---|---|
| Ammonia | $NH_3$ | -34 | -77.7 | 17 | 1357 | 681 |
| Water | $H_2O$ | 100 | 0.0 | 18 | 2258 | 1000 |
| Methanol | $CH_3OH$ | 65 | -97.0 | 32 | 1102 | 791 |
| Ethanol | $C_2H_5OH$ | 79 | -114.3 | 46 | 842 | 789 |

## 2.4 Adsorption of Ammonia on Carbon

Apart from the temperature and pressure of the adsorbate for an adsorption pair, the adsorption of ammonia on wood charcoal also depends on the characteristics of the adsorbent. The characteristics of wood charcoal that leads to adsorption has already been discussed in section 2.2. Inherent properties of charcoal such as specific surface area, carbon-oxygen surface group, porosity and the vast electron cloud over the entire structure contribute to the adsorption of any adsorbate. The carbon-oxygen groups aid in adsorbing ammonia as ammonia is a basic compound and the carbon-oxygen groups are acidic group.

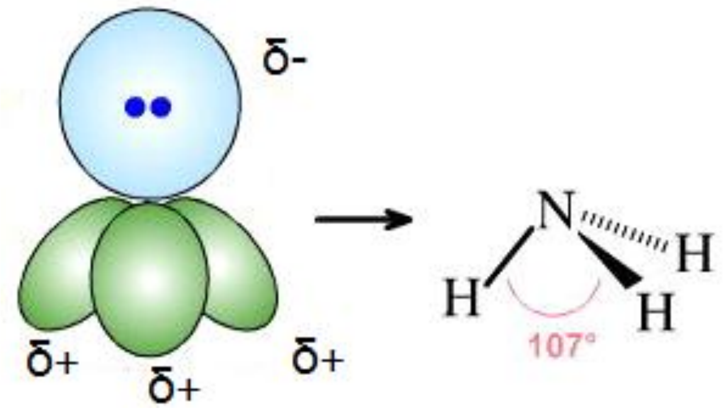

Figure 2.2 Structure of ammonia with lone electrons on the top edge of trigonal pyramid

Ammonia is a compound consisting one atom of nitrogen and three atoms of hydrogen. Since three electrons in the outer shell are used for bonding with hydrogen, another two electrons remain in the outer shell. Such electrons are called lone electrons. According to the valence shell electron pair repulsion theory, ammonia will form a trigonal pyramidal shape. With lone electrons at one end of the trigonal pyramidal shape, it contributes to the dipole of the molecule causing ammonia to be a polar molecule. Thus, ammonia has strong polarity on itself and it can be attracted by either positive poles or negative poles. The structure of wood charcoal which resembles graphite allows ammonia to be attracted to the vast electron cloud which acts as negative poles. Therefore, physical bonding via van der Waals force exists between ammonia and wood charcoal.

In the Dubinin-Radushkevich equation (equation 2.3 and 2.4), parameters D, $\mathbf{k}$, $x_o$, $v_o$ and n differs even with the same adsorption pair. For example, ammonia-activated carbon pair, $x_o$ can vary from 0.2303 to 0.8392 depending on the properties of activated carbon, ranging from its origins, size of particle, method of preparation, method of activation, structure of particle to physical inherent properties such as porosity, density and pore size distribution. Though much research work has been carried out on the adsorption characteristics of carbon, no one has yet determine the parameters in Dubinin-Radushkevich equation for an arbitrary sample. As the scope of this research focuses on the thermodynamic cycle of an adsorption refrigeration cycle, in-depth study of ammonia adsorption on wood charcoal or activated carbon is beyond the scope of this research. Nevertheless, values of k, $x_o$ and n for various types of activated carbon can be found from various journals. These values are therefore tabulated in Table 2.2.

Table 2.2 Characteristics of granulate carbon adsorbent in Dubinin-Radushkevich equation.

| **Author (s)** | **Author's Material code** | $x_o$ | **k** | n | **Origins** |
|---|---|---|---|---|---|
| Tamainot-Telto, et al., 2009 | 208C | 0.3077 | 4.4390 | 1.187 | Wood, coconut shell |
| | 607C | 0.3475 | 3.5943 | 1.05 | Wood, coconut shell |
| | C119 | 0.2852 | 3.8615 | 1 | Wood, coconut shell |
| | SRD1352/2 | 0.8392 | 5.0775 | 0.8529 | Wood, coconut shell |
| | SRD1352/3 | 0.5691 | 6.6738 | 1.1489 | Wood, coconut shell |
| | SRD06038 | 0.4464 | 6.7116 | 1.1295 | Coal |
| | SRD06039 | 0.4527 | 5.3630 | 1.053 | Coal |
| | SRD06040 | 0.3483 | 5.5936 | 1.1714 | Coal |
| | SRD06041 | 0.2303 | 5.5622 | 1.5252 | Coal |
| Wang, et al., 2009 | YKAC | 0.29 | 3.57 | 1.38 | Wood, coconut shell |
| Tamainot-Telto, et al., 2003 | - | 0.3837 | 4.2436 | 1 | - |

From Table 2.2, granulate carbon made of wood has $x_o$ value ranging from 0.2303 to 0.8392, **k** value ranging from 3.5943 to 6.6738 and n value ranging from 0.8529 to 1.525. Granulate carbon made of coal has $x_o$ value ranging from 0.2303 to 0.4527, **k** value ranging from 5.3630 to 6.7116 and n value ranging from 1.053 to 1.5252. These values are important in the design stage for an adsorption refrigeration cycle which will be discussed further the later chapter of this thesis. As shown here, the values of $x_o$, **k**, and n for wood-based carbon have larger range than coal-based carbon. This shows the wood-based carbon disperse more than the coal-based carbon. To date, researchers have yet to explain the behaviour of such trend found in activated carbons. Characterizing active carbon would be difficult due to its random arrangement of the layers and formation of voids during carbonization process but such characterization is not impossible. The major difference between wood and coal based activated carbon is the history of the raw material itself. While coal is a result of oxidization, biodegradation and compaction for a long period of time, wood is harvest after only a few decades from live plants. Nevertheless, in-depth description of the difference between activated carbon made of coal and wood charcoal is not the focus of this research.

The work of Lee and Reucroft (1999a; 1999c), on ammonia adsorption on wood based chemically activated carbons proposed that the adsorption on ammonia is not just physical adsorption. They concluded that that the presence of carbon-oxygen surface function group helps the adsorption of ammonia. Hydrogen atoms in ammonia can interact strongly with oxygen due to high electrostatic attraction. Furthermore, such hydrogen bonding, (N-H···O), has been reported to have energy of 12.55 kJ mol$^{-1}$ (Mortimer, 1983). Hydrogen atoms in ammonia preferably adsorb on specific sites such as carbon-oxygen surface group rather than pure carbon sites. Such "preference" will result in higher energy release. Results of the work of Lee and Reucroft (1999a and 1999c) for wood based chemically activated carbon is shown in Table 2.3. Literature shows much more research on wood based activated carbon rather than wood charcoal and information of ammonia adsorption on wood charcoal is rare. Nevertheless, data from wood based activated carbon shall suffice for comparison.

Table 2.3 Characteristics and adsorption energy for ammonia on chemically activated carbon

| **Sample no.** | **BET surface area, m$^2$ g$^{-1}$** | **Treatment temperature, °C** | **Average micropore, nm** | **Micropore volume, cc g$^{-1}$** | **Ammonia adsorption energy, kJ mol$^{-1}$** | **Composition (at%)** |
|---|---|---|---|---|---|---|
| 6 | 783 | 300 | 1.49 | 0.37 | 33.2 | 77.4% C, 22.5% O and 0.2% P |
| 7 | 1075 | 350 | 1.66 | 0.38 | 29.1 | 83.7% C, 15.5% O and 0.8% P |
| 8 | 1807 | 450 | 2.10 | 0.39 | 24.1 | 83.7% C, 15.5% O and 0.8% P |

Adsorbents with higher surface area generally adsorb more adsorbate due to higher adsorption capacity but ammonia adsorption shows reverse effect as reported by Lee and Reucroft (1999c) & Lee et al. (2005). In their work, the amount of ammonia adsorbed on carbon with higher surface area is less than the carbon with lower surface area and is shown in Figure 2.3. The degree of surface area or microporosity development and the micropore volume does not seem to control ammonia adsorption behaviour (Lee and Reucroft, 1999a and Huang et al., 2008). Surface chemistry, as discussed earlier can explain the trend shown in ammonia adsorption at low relative pressure. In their work, Lee and Reucroft (1999a), lower surface sample contains higher densities of carbon-oxygen surface groups shows higher amount adsorb. Oxygen in the surface functional group provide specific adsorption sites for ammonia adsorption at the low relative pressure range.

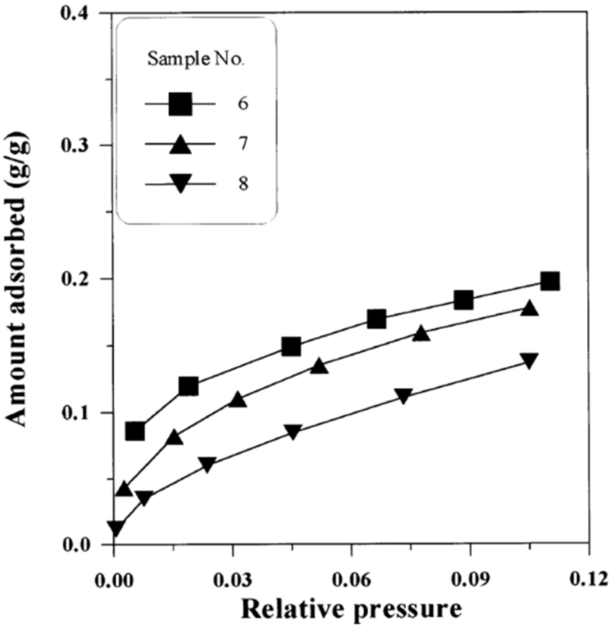

Figure 2.3 Ammonia adsorption of chemically activated wood based carbon at relative low pressure

## 2.5 Ammonia-Activated Carbon Adsorption Refrigeration

The first absorption refrigeration was invented by Ferdinand Carre in 1860. The absorption system used water and ammonia for absorbent and refrigerant respectively. In the 1880s, vapour compression refrigeration gained popularity over the absorption cycle due to its cooling performance and simplicity of the cycle. Development of smaller compressors, automatic refrigerant controls, better shaft seals, developments in electrical power systems and induction motors helped vapour compression systems surpass absorption system in popularity. However, adsorption refrigeration systems have received much attention since 1990s when Montreal Protocol identified CFCs, halons and other halogenated CFCs as threats to ozone layer depletion. The shift from conventional vapour compression to adsorption systems is because the latter systems use environmental friendly refrigerants like ammonia, methanol, water, ethanol and others. Absorption and adsorption systems differ by the way refrigerant absorb in adsorption process. While absorption refers to molecules of gases or liquids which dissolve in another liquid or solid, adsorption refers to gases or liquids which adhere to the surface of solids. Furthermore, adsorption is a surface phenomenon which, in principle, occurs at any pressure and temperature while absorption is a bulk or volume phenomenon which may or may not occur at given pressure and temperature.

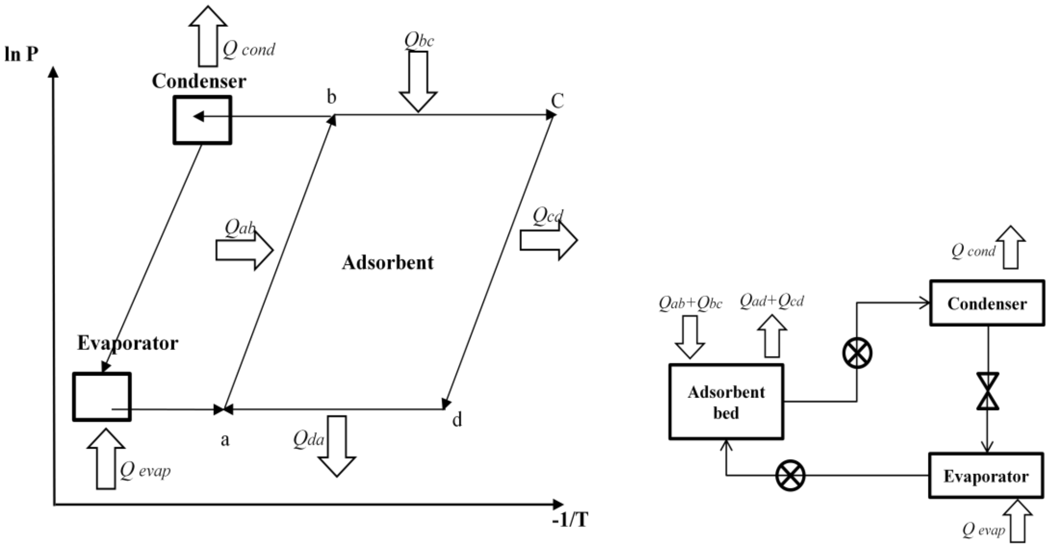

A B

Figure 2.4 Thermodynamic cycle of a basic adsorption refrigeration. A, P-T-x diagram and B, Schematic diagram.

The basic adsorption refrigeration consists of four steps divided into two cycles (Qu, 2002 and wang et al. 2006b). The first cycle is desorption and condensation while another is adsorption and evaporation. As shown in Figure 2.4, the adsorption refrigeration cycle goes through process ab (isosteric heating), bc (isobaric heating), cd (isosteric cooling) and da (isobaric adsorption).

*Process a-b: Isosteric heating*. Valves between adsorbent bed to condenser and evaporator is closed and heated by external source. The temperature of the bed rises from $T_a$ to $T_b$. No desorption occurs in this heating, there is no increment of refrigerant in adsorbent bed. The amount of heat to increase the temperature is the amount of heat to heat up the bed and the adsorbent (wood charcoal or activated carbon) with adsorbate (ammonia) adsorbed. Heat added into the adsorbent bed, $Q_{ab}$, can be determined from:-

$$Q_{ab} = \int_{T_a}^{T_b} \left[ m_{AC} \left( C_{p,AC} + x_{ab} C_{p,NH_3} \right) + m_{bed} C_{p,bed} \right] dT \qquad (2.7)$$

*Process b-c: Isobaric heating*. Heating process is continued even after isosteric heating is completed. A valve between adsorbent bed and condenser is opened. This allows desorption in adsorbent bed and refrigerant is allowed to flow into the condenser where it will be condensed. The pressure during this step remains constant. Apart from heating the bed, heat is also utilized to provide heat for desorption, i.e. heat of desorption. Therefore the total heat added into the system, $Q_{bc}$, can be determine from:-

$$Q_{bc} = \int_{T_b}^{T_c} \left[ m_{AC} \left( C_{p,AC} + x_{bc} C_{p,NH_3} \right) + m_{bed} C_{p,bed} \right] dT + \int_b^c m_{NH_3} \, \Delta H \, dx \qquad (2.8)$$

*Process c-d: Isosteric cooling*. The valve between condenser and adsorbent bed is closed and the temperature of adsorbent bed ($T_c$), which is the maximum temperature of the cycle, is decreased to $T_d$. During this process, both temperature and pressure decreased to evaporator conditions. Heat to be extracted out, $Q_{cd}$, is given as:-

$$Q_{cd} = \int_{T_c}^{T_d} \left[ m_{AC} \left( C_{p,AC} + x_{cd} C_{p,NH_3} \right) + m_{bed} C_{p,bed} \right] dT \qquad (2.9)$$

*Process d-a: Isobaric adsorption*. The valve between the adsorbent bed and evaporator is opened. Vaporization of the adsorbate takes place in the evaporator. Evaporated refrigerant then enters adsorbent bed whereby it is adsorbed. Adsorption of refrigerant releases heat of adsorption which will be required to remove from the adsorbent bed. The temperature of adsorbent-adsorbate pair and the bed should be decreased to $T_a$. In the method used by Qu et al. (2001) and Wang et al. (2002), they adopted the same value for heat of adsorption and heat of desorption. Thus, total heat to be removed, $Q_{da}$, from the bed is given as:-

$$Q_{da} = \int_{T_d}^{T_a} \left[ m_{AC} \left( C_{p,AC} + x_{da} C_{p,NH_3} \right) + m_{bed} C_{p,bed} \right] dT + \int_d^a m_{NH_3} \, \Delta H \, dx \qquad (2.10)$$

Amount of heat to be removed from the condenser, $Q_{cond}$, during condensation can be determined from:-

$$Q_{cond} = m_{NH_3}(\boldsymbol{h}_{enter} - \boldsymbol{h}_{leaving}) \tag{2.11}$$

Consequently, amount of heat removed from the cooling space, $Q_{evap}$, can be determined from:-

$$Q_{evap} = m_{NH_3}(\boldsymbol{h}_{enter} - \boldsymbol{h}_{leaving}) \tag{2.12}$$

The coefficient of performance for refrigeration cycle can be determined from:-

$$COP = \frac{Q_{evap}}{Q_{ab}+Q_{bc}} \tag{2.13}$$

Specific cooling power is another term to describe the effectiveness of an adsorption refrigeration cycle. It is define as the ratio of cooling power to the mass of adsorbent.

$$SCP = \frac{Q_{evap}}{m_{adsorbent}} \tag{2.14}$$

As the process described earlier, adsorption refrigeration system suffers from the interval working principles while vapour compression system is a continuous cycle. This is the reason specific cooling power was introduced for an adsorption cooling system. Moreover, mass of adsorbent is another additional mass compared to vapour compression system while keeping in mind the common comparable mass in both system such as mass of evaporator, condenser, pipes and additional accessories such as accumulator. Hence, mass of adsorbent and the adsorber-desorber tank has to counter the mass of compressor for competiveness. Another disadvantage of the adsorption system is the heat transfer in the adsorber-desorber tank. Due to the porosity of the adsorbent, heat transfer is greatly reduced. Such reduction in heat transfer causes more heat to be added into the system to provide a substantial heat compression to a higher pressure for a certain cooling capability. Thus it affects the COP of adsorption system severely. From the literature reviews, COP of adsorption systems are usually less than one. However, COP for vapour compression systems are always greater than one. Performance and cooling power of various ammonia-activated carbon refrigeration systems from literature of the past decade is tabulated in Table 2.4. From Table 2.4, specific cooling power range from 0.06 to 1.0 kW kg$^{-1}$ for ammonia-activated carbon adsorption system. Specific cooling power for most of the system falls within 0.5 kW kg$^{-1}$. The cooling power of adsorption refrigeration using ammonia-activated carbon is in the range of 0.30 to 4.00 kW with cycle times ranging from three to 60 minutes. In addition, COP for adsorption refrigeration using ammonia-activated carbon range from 0.09 to 1.12. The COP of most of these systems is approximately 0.30.

Table 2.4 Performance and capability of various ammonia-activated carbon adsorption refrigeration systems

| **Author (s)** | **Method** | **Type** | **COP** | **SCP, kW $kg^{-1}$** | **Cooling Power, kW** | **Cycle Time, mins** |
|---|---|---|---|---|---|---|
| Tamainot-Telto et al. (2009) | Simulation | Monolithic carbon | 0.3-0.6 | - | - | - |
| | Simulation | Granular carbon | 0.2-0.7 | - | - | - |
| | Simulation | Carbon fiber | 0.1-0.6 | - | - | - |
| | Simulation | Carbon powder | 0.1-0.7 | - | - | - |
| | Simulation | Compacted carbon | 0.1-0.7 | - | - | - |
| Wang et al. (2006b) | Experiment | With mass recovery | 0.25 | 0.473 | 0.89 | 30 |
| | Experiment | With mass recovery | 0.31 | 0.579 | 1.09 | 40 |
| | Experiment | With mass recovery | 0.34 | 0.627 | 1.18 | 50 |
| | Experiment | With mass recovery | 0.32 | 0.595 | 1.12 | 60 |
| | Experiment | Without mass recovery | 0.16 | 0.303 | 0.57 | 30 |
| | Experiment | Without mass recovery | 0.19 | 0.361 | 0.68 | 40 |
| | Experiment | Without mass recovery | 0.22 | 0.420 | 0.79 | 50 |
| | Experiment | Without mass recovery | 0.21 | 0.388 | 0.73 | 60 |
| Wang et al. (2006a) | Experiment | | 0.24 | 0.494 | 0.93 | 30 |
| | Experiment | | 0.30 | 0.563 | 1.06 | 40 |
| | Experiment | | 0.36 | 0.627 | 1.18 | 50 |
| | Experiment | | 0.35 | 0.595 | 1.12 | 60 |
| Oliveira et al. (2007) | Experiment | | 0.35 | 1.000 | - | - |
| Critoph (1999) | Simulation | | 0.67-1.12 | 0.178-0.557 | - | - |
| Lambert & Jones (2006b) | Calculation | Highway cruise | 0.46 | 0.306 | 2.00 | 6.7 |
| | Calculation | City cruise | 0.50 | 0.510 | 3.33 | 6.7 |
| | Calculation | Idle | 0.83 | 0.610 | 4.00 | 6.7 |
| Tamainot-Telto & Critoph (2003) | Experiment | Basic | 0.22 | 0.220 | 0.55 | 10 |
| | Experiment | 0.125 mm fin | 0.20 | 0.580 | 1.50 | 3.33 |
| | Experiment | 0.300 mm fin | 0.21 | 0.400 | 1.06 | 5 |
| Qu, et al. (2002) | Experiment | | 0.09-0.13 | 0.060 | 2.00 | 34-46 |
| Vasiliev, et al. (2001) | Experiment | | 0.75 | - | 0.30 | 12 |

Vasiliev et al. (2001) designed and study a solar-gas solid sorption using ammona-activated carbon fiber adsorption pair for the heat pump. They used two different types of heat source; which is gas flame and solar. Solar collector sized

3 m$^2$ was used in the solar adsorption system. Heat sources was maintained at 1 kW for comparison. The cooling output was approximately 750 W which in turn gave a COP of 0.75. Both heat sources, either flame or solar, was experimentally tested. The cycle time for the system was limited to 12 minutes due to the limitation of the activated carbon fiber material.

Qu et al. (2002) constructed an adsorption refrigeration system using ammonia-activated carbon as the working pair. They simulate two types of cycles with ammonia-activated carbon where they believe mass recovery system will have better performance than the basic one. From their simulation, they found out that the mass recovery system has lower COP in the desorption temperature range 120 to 160 °C. COP for both system are approximately similar to each other in the temperature region of 180 to 230 °C. COP of both system reported to be in between 0.07 to 0.16. With the experiment setup, COP was found in the range of 0.09 to 0.13 with cycle time of 34 to 46 minutes. SCP was in the range of 0.060 to 0.069 kW kg$^{-1}$.

Tamainot-Telto & Critoph (2003) designed three small experimental adsorption air conditioning modules using ammonia-monolithic carbon pair. The three variants were related with the construction of the heat transfer fins. Initially, a basic construction of the module was done without fins. The other two modules were produced with fins of 0.125 mm thickness and 0.300 mm. The module with 0.125 mm fins gave better heat transfer properties therefore better performance in terms of cooling output. It gave about twice the cooling production of the basic module and 40% higher than the module with 0.300 mm fin thickness. All three systems had a similar COP.

Lambert and Jones (2006a and 2006b) analyzed heat from exhaust gas from an automobile at three different drive conditions; namely idling, city cruise and highway cruise. Then, they design an air conditioning system using adsorption system for the driving condition of the automobile with exhaust gas as the heat source. Heating source was found to increase from idling to highway cruise due to the exhaust power increases as these conditions. In their design, they utilize ammonia-activated carbon fiber as the adsorption pair for the air conditioning purpose. They use an analytical method to design the system. In their work, they targeted to cool the car cabin within 6.7 minutes. In their design, there were three adsorber-desorber cylinders for the adsorption air conditioner. While two are utilize for heating (ammonia desorption) and cooling (ammonia adsorption), the third was left to cool down after the desorption process from the previous cycle. This intermittent cylinder is preparing for adsorption of ammonia in the next cycle. Results from their analyses are shown in Table 2.4.

Critoph (1999) wrote a simplified thermodynamic Mathlab model to predict the COP of a convective thermal wave cycle for ammonia-granular activated carbon adsorption refrigeration system. In his model, he varied four parameters to study the effects of each parameter on the system. The parameters varied are bed length, heat transfer fluid’s flow rate, breakthrough temperature and initial isothermal temperature. COP is found to increase as bed length and initial temperature increases while COP was found to be reduce as the heat transfer fluid’s flow rate increase. Increment of breakthrough temperature does not seem to have effect on the COP of his system modelled. Using suitable parameters, the author then streamed down to design an air conditioning unit using a highly adsorbent carbon with high heat transfer coefficient. However, no experimental data was presented.